Molecular Crystals and Liquid Crystals
Publication details, including instructions for authors and subscription information:
http://www.tandfonline.com/loi/gmcl16

The Planar Deformation Behavior of Skinned Striated Muscle Fibers

Raymond J. Hawkins [a b] & Ernest W. April [a]
[a] Department of Anatomy and Cell Biology, College of Physicians and Surgeons, Columbia University, New York, New York, 10032
[b] Henry Krumb School of Mines, Columbia University, New York, New York, 10027
Version of record first published: 20 Apr 2011.

To cite this article: Raymond J. Hawkins & Ernest W. April (1983): The Planar Deformation Behavior of Skinned Striated Muscle Fibers, Molecular Crystals and Liquid Crystals, 101:3-4, 315-328

To link to this article: http://dx.doi.org/10.1080/01406568308072539

Mol. Cryst. Liq. Cryst., 1983, Vol. 101, pp. 315–328
0026-8941/83/1014–0315/$18.50/0

Printed in the United States of America

The Planar Deformation Behavior of Skinned Striated Muscle Fibers

RAYMOND J. HAWKINS† and ERNEST W. APRIL

Department of Anatomy and Cell Biology, College of Physicians and Surgeons, Columbia University, New York, New York 10032

(*Received September 27 1982; in final form July 8, 1983*)

The osmotically produced planar deformation behavior of skinned striated muscle fibers (smectic B_1 lattice microstructure) is investigated using light microscopy and compared with analogous results determined using x-ray diffraction. The nonlinear pressure-volume relationship measured using light microscopy is shown to be essentially the same as that resultant of similar experiments using x-ray diffraction. The application of a continuum analysis based on the Murnaghan equation of state to this deformation behavior is examined. The Murnaghan equation is shown to approximate well the nonlinear planar deformation behavior of these muscle fibers.

INTRODUCTION

In earlier communications[1,2] a continuum analysis was introduced to treat the planar deformation behavior of skinned striated muscle fibers measured by x-ray diffraction. Here this deformation is restricted to the plane perpendicular to the director of the myosin-rod lattice, i.e., to the cross sectional area of the lattice. Similar planar deformation behavior can also be observed by light microscopy. Whether these two techniques give essentially similar information concerning the planar deformation behavior of skinned striated muscle fibers is currently a

†Present Address: Henry Krumb School of Mines, Columbia University, New York, New York 10027

controversial issue. An attempt to quantitatively correlate the planar deformation behavior of skinned striated muscle fibers resultant from these two techniques had yet to be undertaken. As a first step towards resolving this dispute, we have undertaken a series of experiments parallel to our original x-ray studies using light microscopy. Further, these analyses are accomplished for three different structural conditions in which the interstitial concentration in the myosin-rod lattice of the muscle fiber is markedly different. The nonlinear pressure-volume relationship of these fibers is analyzed, as before[1,2] using the Murnaghan equation.[3] Subsequent to our original treatment using the Murnaghan equation, questions concerning the appropriateness of the Murnaghan equation had arisen because the skeletal muscle fibers under investigation are optically anisotropic. Extension of the analysis using the Murnaghan equation to this data requires that the planar elastic properties of anisotropic (especially hexagonal) media under our experimental conditions be isotropic. To this end, we analyze the elastic properties of appropriately oriented anisotropic media under plane-strain pure-hydrostatic conditions and show them to be isotropic in the plane perpendicular to the major symmetry axis (Appendix A).

The striated muscle fiber with the limiting membrane removed can be considered a stack of multidomain SmB_1 myosin-rod liquid-crystalline monolayers. The director of each monolayer is coincident with the long axis of the muscle fiber. The two-dimensional space group of the myosin-rod lattice is *p6mm*[4]. The separation of the monolayers along the length of the fiber is quite uniform. These monolayers are connected longitudinally, one to another, via interstitial filaments composed primarily of actin. (In the interest of clarity we use the terms 'rod' and 'filament' to denote myosin and actin structures, respectively.) At the interstitial sites of the myosin-rod lattice of crayfish muscle, the actin filaments penetrate into the myosin-rod monolayer at both ends in a 6 : 1 unit-cell ratio. The myosin-rod lattice together with the interdigitating filaments appear to fulfill the orientational requirements of an *interstitial solid-solution*. The longitudinal intermonolayer distance and depth of actin-filament interdigitation (concentration of actin in the myosin-rod lattice) are linearly dependent upon the degree of muscle shortening (sarcomere length) which may be experimentally altered by mechanical application of tension along the long axis of the muscle fiber. This feature was used to vary the interstitial concentration of the myosin-rod lattice. The layer thickness of the myosin-rod lattice (equivalent to the length of a myosin rod) does not change during osmotic compression.

MATERIALS AND METHODS

Procedures followed in the light microscopy experiments parallel those of our earlier x-ray work. Single long tonic muscle fibers were dissected from the meropodite of the walking leg of the crayfish (*Orconectes*), stripped of the surrounding fiber membrane as previously described[5,6,7] and checked for cylindrical uniformity. These skinned muscle fibers were mounted in plexiglass chambers on an inverted Nikon M2 microscope. The diffraction of light (0.3 mW He—Ne laser) was used to monitor the sarcomere length as previously reported.[5] Fiber diameters were measured either with a filar micrometer or from photomicrographs. Osmotic pressure was applied to the

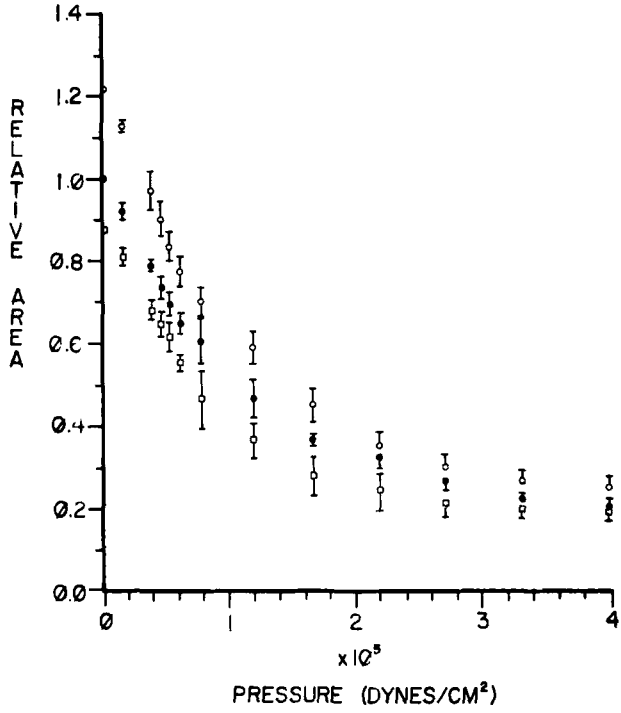

FIGURE 1 Relative area plotted as a function of pressure at three actin concentrations. Increasing the sarcomere length decreases the actin concentration in the myosin-rod lattice. The zero-pressure relative cross-sectional areas are normalized to the relative cross-sectional area determined at the mean physiological equilibrium actin concentration (46%). This zero-pressure correction factor was then used to renormalize the higher pressure data. The open circles denote a sarcomere length of 7.26 micrometers, the solid circles a sarcomere length of 9.68 micrometers, and the open squares a sarcomere length of 11.09 micrometers. The bars denote the standard deviation of the mean.

muscle fibers by introducing polyvinylpyrrolidone (PVP-10, MW = 10,000 g/mol) into the bathing solutions.[8-10] The calculated pressures are (a) very close to those obtained when muscle fibers with intact surrounding membranes are used as osmometers,[8] (b) similar to those reported by other investigators,[11,12] and (c) consistent with high precision experiments carried out on a slightly different preparation of PVP-10.[13] Data was collected for skinned muscle fibers in the relaxed state at three different sarcomere lengths (Figure 1). All experiments were carried out at room temperature. The bathing solutions were composed of 200 mM potassium propionate, 5 mM $MgCl_2$, 9 mM K_2EGTA, 1 mM calcium propionate, 1 mM ATP and buffered to pH 7 with 20 mM Tris.[14] In all experiments the incremental changes in applied pressure were small enough to ensure that there was no measurable loss of lattice cohesive energy.

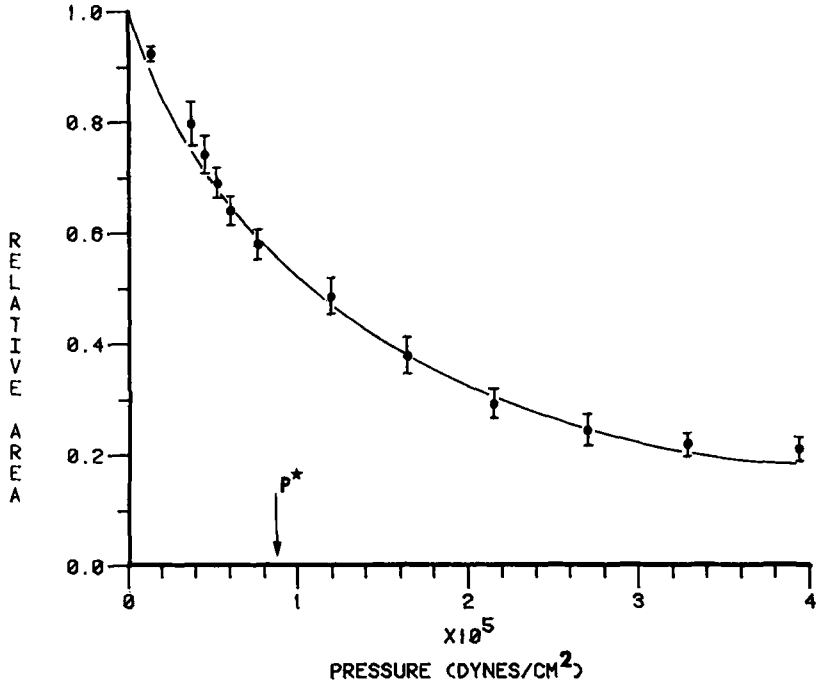

FIGURE 2 The effect of pressure on the relative fiber area at a sarcomere length of 7.26 micrometers. The curve represents the least-squares fit of the Murnaghan equation. The bars denote the standard deviation of the mean. P^* ($= 8.86 \times 10^4$ dynes/cm^2) indicates the limit of the cubic polynomial.

RESULTS AND ANALYSIS

The analysis of the pressure-volume data obtained from a typical striated muscle fiber compression experiment requires an equation of state capable of accommodating large deformations. Such an equation is the Murnaghan equation:[3]

$$P = \left(K_0/K_0'\right)\left[\left(V_0/V\right)^{K_0'} - 1\right] \tag{1a}$$

where K_0 is the isothermal bulk modulus and K_0' its pressure derivative.

While the A-band of striated muscle is optically anisotropic (whence its name) due to the 3-dimensional arrangement of the myosin-rod

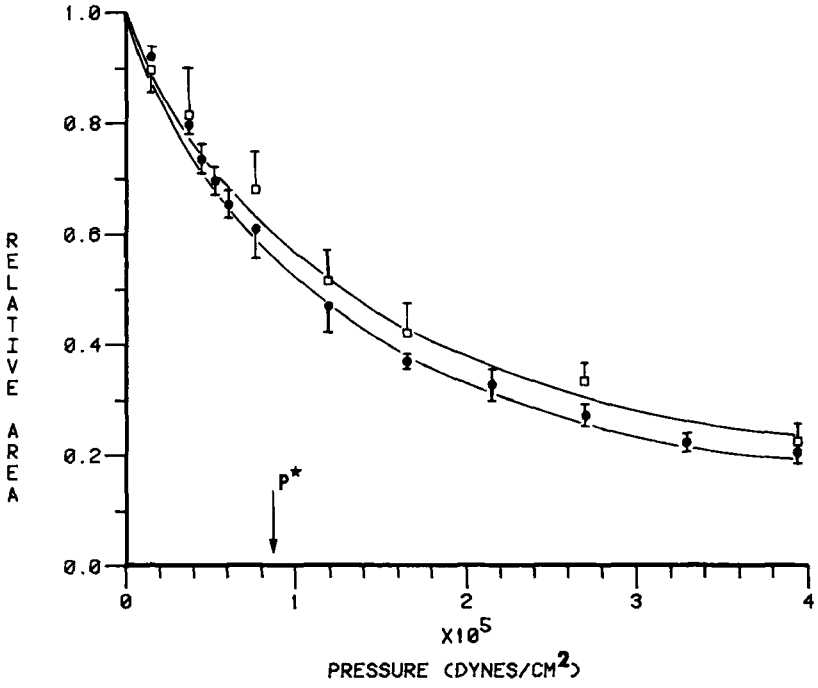

FIGURE 3 The effect of pressure on the relative fiber area measured using light microscopy at a sarcomere length of 9.68 micrometers (circles) and the relative unit-cell area measured using x-ray diffraction at a sarcomere length of 9.61 micrometers (squares). The curves represent the least-squares fit of the Murnaghan equation. The bars denote the standard deviation of the mean. P^* indicates the limit of the cubic polynomial for the light microscope data ($P^*_{LM} = 8.69 \times 10^4$ dynes/cm^2, $P^*_{\text{X-RAY}} = 8.49 \times 10^4$ dynes/cm^2).

lattice, in these studies the deformation is restricted to the cross-sectional area of the myosin lattice (the plane perpendicular to the director). In this plane and under our experimental conditions, as demonstrated in Appendix A, the elastic properties are *isotropic*. Thus, the use of an expression such as the Murnaghan equation is, in these experiments, justified. Since we have taken the z-axis to be of constant length, we may rewrite the Murnaghan equation in the following working form:

$$P = (K_0/K_0')\left[(A_0/A)^{K_0'} - 1\right] \tag{1b}$$

where A denotes the cross-sectional area.

The pressure-volume behavior of skinned striated muscle fibers at three sarcomere lengths was measured using light microscopic meth-

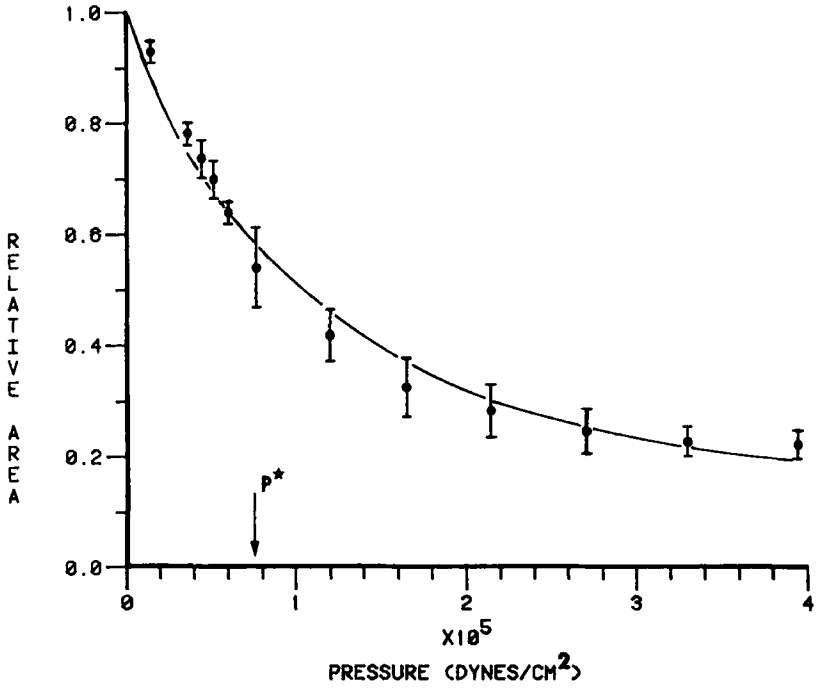

FIGURE 4 The effect of pressure on the relative fiber area at a sarcomere length of 11.09 micrometers. The curve represents the least-squares fit of the Murnaghan equation. The bars denote the standard deviation of the mean. P^* ($= 7.56 \times 10^4$ dynes/cm^2) indicates the limit of the cubic polynomial.

TABLE I

Comparison between experimental relative areas measured using light microscopy and those generated by the Murnaghan equation (sarcomere length = 7.26 μm)

Number of Observations	Applied Pressure (dynes/cm^2)	Experimental A/A_0	Std. Dev.	Generated A/A_0
3	1.44×10^4	0.923	0.011	0.898
3	3.68×10^4	0.796	0.041	0.769
3	4.44×10^4	0.740	0.032	0.732
3	5.21×10^4	0.688	0.028	0.697
3	6.01×10^4	0.640	0.025	0.664
3	7.65×10^4	0.579	0.028	0.603
3	1.19×10^5	0.484	0.032	0.481
3	1.65×10^5	0.375	0.031	0.388
3	2.15×10^5	0.291	0.027	0.316
3	2.70×10^5	0.246	0.026	0.259
3	3.29×10^5	0.219	0.023	0.213
3	3.94×10^5	0.210	0.023	0.177

ods over a pressure range of 0 to 3.94×10^5 dynes/cm^2. The values of K_0 and K_0' were determined using the grid search method described in Appendix B.

The behavior of these fibers under compression at three different sarcomere lengths (i.e. different concentrations of actin in the myosin-rod lattice) is shown in Figures 2 to 4. The curves are generated from the values of K_0 and K_0'. The experimental and generated behavior are compared in Tables I–IV. The values of K_0, K_0' and relevant statistics are given in Table V.

TABLE II

Comparison between experimental relative areas measured using light microscopy and those generated by the Murnaghan equation (sarcomere length = 9.68 μm)

Number of Observations	Applied Pressure (dynes/cm^2)	Experimental A/A_0	Std. Dev.	Generated A/A_0
3	1.44×10^4	0.918	0.022	0.898
3	3.68×10^4	0.794	0.015	0.772
3	4.44×10^4	0.735	0.027	0.735
3	5.21×10^4	0.696	0.026	0.701
3	6.01×10^4	0.650	0.029	0.668
3	7.65×10^4	0.607	0.056	0.608
3	1.19×10^5	0.468	0.046	0.488
3	1.65×10^5	0.371	0.016	0.395
3	2.15×10^5	0.327	0.024	0.323
3	2.70×10^5	0.271	0.019	0.266
3	3.29×10^5	0.222	0.016	0.221
3	3.94×10^5	0.205	0.021	0.184

TABLE III

Comparison between experimental relative areas measured using light microscopy and those generated by the Murnaghan equation (sarcomere length = 11.09 μm)

Number of Observations	Applied Pressure (dynes/cm^2)	Experimental A/A_0	Std. Dev.	Generated A/A_0
3	1.44×10^4	0.926	0.020	0.893
3	3.68×10^4	0.780	0.021	0.762
3	4.44×10^4	0.738	0.032	0.724
3	5.21×10^4	0.701	0.037	0.690
3	6.01×10^4	0.636	0.023	0.656
3	7.65×10^4	0.537	0.073	0.597
3	1.19×10^5	0.421	0.047	0.478
3	1.65×10^5	0.323	0.054	0.389
3	2.15×10^5	0.284	0.049	0.320
3	2.70×10^5	0.247	0.041	0.266
3	3.29×10^5	0.228	0.026	0.223
3	3.94×10^5	0.223	0.026	0.188

DISCUSSION

As demonstrated in Figures 2 to 4, the nonlinear behavior of mechanically skinned striated muscle fibers with respect to compression as determined by light microscopy is approximated well by the Murnaghan equation. Detailed discussion concerning the Murnaghan equation is given elsewhere.[1-3,15] Nevertheless, subsequent to our original use of the Murnaghan equation, questions concerning its

TABLE IV

Comparison between experimental relative areas measured using X-ray diffraction[2] and those generated by the Murnaghan equation (sarcomere length = 9.61 μm)

Number of Observations	Applied Pressure (dynes/cm^2)	Experimental A/A_0	Std. Dev.	Generated A/A_0
4	1.44×10^4	0.891	0.038	0.909
5	3.68×10^4	0.808	0.086	0.794
5	7.65×10^4	0.682	0.068	0.645
1	1.19×10^5	0.518	0.053[a]	0.532
13	1.65×10^5	0.425	0.055	0.445
6	2.70×10^5	0.335	0.035	0.319
3	3.94×10^5	0.226	0.037	0.235

[a]Since only one measurement was obtained at this pressure this value represents an estimated standard deviation obtained by taking the arithmetic mean of the other standard deviations.

TABLE V

The isothermal bulk modulus (K_0) and its pressure derivative (K_0') at various sarcomere lengths

Sarcomere length (micrometers)	K_0 (10^5 dynes/cm^2 ± Std. Dev.)	K_0' (± Std. Dev.)	χ_ν^2
7.26	1.30 ± 0.04	0.60 ± 0.06	1.08
9.61	1.46 ± 0.12	0.79 ± 0.14	0.21
9.68	1.31 ± 0.03	0.63 ± 0.05	0.68
11.09	1.22 ± 0.05	0.71 ± 0.08	1.08

χ_ν^2 = reduced chi square for the fit.

relation to polynomials have been raised. The superior applicability of the Murnaghan expression over second and higher order polynomial equations has been discussed in depth by Anderson.[15] By expanding V to fourth order in pressure, Anderson obtained (V/V_0) to the fourth order in (P/K_0) in the form:

$$(V/V_0) = 1 - (P/K_0) + m(P/K_0)^2 - n(P/K_0)^3 + q(P/K_0)^4, \tag{2}$$

where

$$m = m(K_0'), n = n(K_0, K_0', K_0''),$$

and

$$q = q(K_0, K_0', K_0'', K_0''').$$

Anderson[15] contrasted the applicability of the cubic and quartic versions of equation (2) and the Murnaghan equation. As demonstrated in Figures 4 and 7 of Anderson's paper,[15] both the cubic and quartic equations become seriously inadequate. Bridgeman[16] used an expression equivalent to the quadratic extent of equation (2), but found it inadequate for compression data at high pressure. Indeed, while all these expressions (quadratic, cubic, quartic, and Murnaghan) give comparable results over a relatively small range of low pressure, only the Murnaghan equation is capable of following the data over adequately large ranges of pressure. To illustrate this difference we use the expression obtained by Anderson[15] to calculate the upper limit of applicability of the cubic equation:

$$P^* = (3/2)K_0/(1 + 2K_0') \tag{3}$$

These results are indicated in Figures 2, 3, and 4. The quadratic equation becomes inadequate at even lower pressures and the quartic equation becomes inadequate at somewhat higher pressure, diverging greatly from the data at that point. Anderson stressed the importance of P^* as a limit that should be observed when applying the cubic equation: "If data at pressures above P^* are forced into a cubic (equation), the slope of the curve at low pressures will be distorted, leading to erroneous values of the compressibility".[15] The principal merits of the Murnaghan equation are that (1) the elastic constants, K_0 and K_0' are readily extracted from the experimental data and (2) the entire pressure range is describable in terms of only *two* elastic constants.

There is remarkable agreement between the pressure-volume behavior measured using light microscopy and that measured using x-ray diffraction even though the light microscope provides a measure of the compression of the whole muscle fiber including many intracellular components and osmotic compartments apart from the myosin-rod lattice; whereas x-ray diffraction provides an exclusive measure of the myosin-rod lattice compression. Accordingly, we conclude that the light microscope and x-ray diffraction measurements of the planar deformation behavior of these skinned striated muscle fibers are comparable. As demonstrated in Table V, the differences between the values of K_0 and K_0' determined using x-ray diffraction and those determined using light microscopy in the 9.6 micrometer range are not significant. Consequently, these two techniques give essentially the same information concerning planar deformation behavior of these skinned striated muscle fibers even when the intracellular osmotic compartments are not removed.

The differences in the bulk modulus of these skinned striated muscle fibers at the three sarcomere lengths studied appear to be significant. That there is a region of sarcomere length in which no change in bulk modulus is observed is consistent with the findings of Maughan and Godt.[10] At the longest sarcomere length, where the concentration of the interstitial actin is minimized and a different bulk modulus might be expected,[10,17] the bulk modulus is significantly lower.

Much of the previous work[18-21] concerning the myosin-rod lattice has centered on the nature of the intermolecular forces. In those reports, balances involving osmotic, electrostatic, mixing entropic, and other forces have been discussed in relation to lattice stability. Both Millman and Nickel[18] and Maughan and Godt[10,19] have presented detailed discussions concerning the pressure-volume behavior of

skinned striated muscle fibers under conditions similar to those reported here. The utilization of the Murnaghan equation has the important advantage over the analysis of Maughan and Godt[10] in that it is defined over the entire experimental pressure range, and is more general, albeit less specific concerning molecular interactions, than the analysis of Millman and Nickel.[18] Furthermore, our analysis necessitates fewer assumptions about the microstructure of muscle fibers than does that of Maughan and Godt[19] or that of Millman and Nickel.[18] Since the constraints imposed in our treatment (Appendix A) concern only crystal system symmetry, the results may be applied to other muscle systems without regard to myosin-rod dimension, actin-filament dimension, or to the unit-cell ration of actin filaments to myosin rods. This analysis is also applicable to muscle fibers in which the ordered domains of myosin rods are small compared to the fiber width or in which the myosin-rod lattice is characterized by short-range orientational order.

The planar deformation of the skinned striated muscle fiber is reversible provided that the lattice deformation is limited to the elastic region. The data presented here are from fibers that showed no loss in lattice cohesive energy. Since elastic deformation is a common material property, it is unnecessary to evoke secondary elastic structures as suggested by others[10] to account for this behavior. Indeed, a principle advantage of our analysis is that it provides a structural model that is consistent with the known liquid-crystalline microstructure of the striated muscle fiber and a continuum formalism with which the nonlinear elastic behavior may be examined quantitatively.

APPENDIX A

In this analysis we consider only elastic deformation in the plane-strain pure-hydrostatic condition.

When the z axis is of constant length, under plane-strain conditions the non-zero strain tensor components are ϵ_{jk} where $j, k \neq z$. Under pure hydrostatic pressure $\epsilon_{xy} = 0$ for the crystal systems to be examined. Thus the strain tensor assumes the form

$$\epsilon = \begin{bmatrix} \epsilon_{xx} & 0 & 0 \\ 0 & \epsilon_{yy} & 0 \\ 0 & 0 & 0 \end{bmatrix} \tag{A1}$$

As a function of the strain tensor components (ϵ_{jk}) and stiffness tensor components (C_{jklm}), the strain energy density is given by

$$F = (1/2)C_{jklm}\epsilon_{jk}\epsilon_{lm}; \tag{A2}$$

the Einstein summation convention to be understood on repeated indices. Using the form of (A2) subject to the symmetry conditions of the various crystal systems given in Landau and Lifschitz[22] and imposing the constraints of (A1), we obtain the following stiffness dependence of the strain energy density:

$$\left.\begin{matrix}\text{Hexagonal:}\\ \text{Rhombohedral:}\end{matrix}\right\} F = 2C_{\xi\eta\xi\eta}(\epsilon_{xx} + \epsilon_{yy})^2 + C_{\xi\xi\eta\eta}(\epsilon_{xx} - \epsilon_{yy})^2 \tag{A3}$$

$$\left.\begin{matrix}\text{Tetragonal:}\\ \text{Cubic:}\end{matrix}\right\} F = (1/2)C_{xxxx}\left(\epsilon_{xx}^2 + \epsilon_{yy}^2\right) + C_{xxyy}\epsilon_{xx}\epsilon_{yy} \tag{A4}$$

$$\left.\begin{matrix}\text{Orthorhombic:}\\ \text{Monoclinic:}\end{matrix}\right\} F = (1/2)\left(C_{xxxx}\epsilon_{xx}^2 + C_{yyyy}\epsilon_{yy}^2\right) + C_{xxyy}\epsilon_{xx}\epsilon_{yy} \tag{A5}$$

where $\xi = x + iy$, $\eta = x - iy$, and $i = (-1)^{1/2}$. The same result is noted by Landau and Lifschitz[22] for the hexagonal system when ϵ_{xx}, and ϵ_{yy}, ϵ_{xy} are all non-zero. Since the planar deformation of the cubic, hexagonal, rhombohedral, and tetragonal systems is determined by only two stiffness constants, the elastic properties of these crystal systems are isotropic.[22] Although this analysis concerns single crystals, the situation as regards polycrystalline or microcrystalline materials is similar since "polycrystalline bodies whose component crystallites are sufficiently small may be regarded as isotropic bodies".[22] Since the planar microstructure of the muscle fibers in our experiments is dominated by the hexagonal myosin-rod lattice of constant layer thickness and since the planar elastic properties of the hexagonal crystal system are isotropic under plane-strain pure-hydrostatic conditions, the use of an equation of state derived for isotropic materials to describe the planar deformation behavior of these muscle fibers is appropriate.

APPENDIX B

In our previous papers[1,2] K_0 and K_0' were determined using an iterative linear regression algorithm in which a range of K_0' was subdivided and linear regression analysis run for each value of K_0' to determine K_0. The pair (K_0, K_0') giving the best fit were then taken to be the appropriate parameters. This method did not lend itself to estimating the error in K_0' since this parameter was treated as an arbitrary parameter. In the present paper we have used a different least-squares fitting method. Chi square, χ^2, is considered a continuous function of K_0 and K_0' and the 3-D space (χ^2, K_0, K_0') is searched to find the minimum value of χ^2 using a grid-search mapping algorithm.[23] Since we are now using different statistical criteria to determine K_0 and K_0' we have presented the data from our earlier work[2] with the χ^2 fit in Table IV.

Acknowledgment

We thank Jennie Schreder and Paul Ginouves for their technical assistance, Barry W. Millman and Gerald F. Elliott for their evaluations and suggestions, and Robert A. Aldoroty for many helpful discussions. This research was supported in part by grants from the National Institutes of Health (5R01-AM15876) and the Muscular Dystrophy Association.

References

1. R. J. Hawkins and E. W. April, *J. Gen. Physiol.*, **78**, 18a (1981).
2. R. J. Hawkins and E. W. April, *Mol. Cryst. Liq. Cryst.*, **75**, 211–216 (1981).
3. F. D. Murnaghan, *Proc. Nat. Acad. Sci.*, **30**, 244–248 (1944).
4. W. Helfrich, *J. Phys. Coll., Supp. 4*, C3-105-C3-114 (1979).
5. E. W. April, P. W. Brandt, and G. F. Elliott, *J. Cell Biol.*, **51**, 72–82 (1971).
6. E. W. April, P. W. Brandt, and G. F. Elliott, *J. Cell Biol.*, **52**, 52–65 (1972).
7. E. W. April and D. Wong, *J. Mol. Biol.*, **101**, 107–14 (1976).
8. E. W. April and J. Schreder, *Biophys. J.*, **25**, 18a (1979).
9. A. Magid and M. K. Reedy, *Biophys. J.*, **30**, 27–40 (1980).
10. D. W. Maughan and R. E. Godt, *Biophys. J.*, **28**, 391–402 (1979).
11. D. W. Maughan, private communication.
12. B. W. Millman, private communication.
13. H. Vink, *Eur. Polymer J.*, **7**, 1411–1419 (1971).
14. M. Kawai and P. W. Brandt, *J. Gen. Physiol.*, **68**, 267–280 (1976).
15. O. L. Anderson, *J. Phys. Chem. Solids*, **27**, 547–565 (1966).
16. P. W. Bridgman, *Collected Experimental Papers*, (Harvard University Press, 1964), Vol. 1–7.
17. H. J. Goldschmidt, *Interstitial Alloys* (Plenum Press, New York, 1967), Chap. 2, pp. 33.
18. B. W. Millman and B. G. Nickel, *Biophys. J.*, **32**, 49–64 (1981).
19. D. W. Maughan and R. E. Godt, *Biophys. Struct. Mech.*, **7**, 17–40 (1980).

20. E. W. April, *J. Mechanochem. Cell Motility*, **3**, 111–121 (1975).
21. E. W. April, *Mesomorphic Order in Polymers and Polymerization in Liquid-Crystalline Media*, *ACS Symposium Series*, **74**, 248–255 (1978).
22. L. D. Landau and E. M. Lifschitz, *Theory of Elasticity* (Pergamon Press, New York, 1970), 2nd ed., Chap. 1, pp. 37–43.
23. P. R. Bevington, *Data Reduction and Error Analysis for the Physical Sciences* (McGraw-Hill, New York, 1969), Chap. 11, pp. 208.